CrystEngComm

Accepted Manuscript

ROYAL SOCIETY OF CHEMISTRY

www.rsc.org/crystengcomm

CrystEngComm

Dynamic Article Links ►

Cite this: DOI: 10.1039/c6ce00000x

www.rsc.org/CrystEngComm

ARTICLE

Structural Diversity, Luminscence, and Photocatalytic Properties of Six Coordination Polymers Based on Designed Bifunctional 2-(1-imidazol-yl)terephthalic Acid

Xiutang Zhang,*[a,b] Liming Fan,[a,b] Weiliu Fan,[b] Bin Li,[a] Guangzeng Liu,[a] Xinzheng Liu[a] and Xian Zhao*[b]

Received (in XXX, XXX) Xth XXXXXXXXX 2016, Accepted Xth XXXXXXXXX 2016
DOI: 10.1039/c6ce00000x

ABSTRACT: Six coordination polymers (CPs), $\{[M(ITA)]\cdot 0.5H_2O\}_n$ (M=Zn for **1**, M=Mn for **2**), $\{[Zn(ITA)(bib)_{0.5}]\cdot 1.5H_2O\}_n$ (**3**), $\{[Ni(ITA)(bib)_{0.5}(H_2O)_3]\cdot H_2O\}_n$ (**4**), $\{[Zn(ITA)(bimb)_{0.5}]\cdot 0.5H_2O\}_n$ (**5**), and $[Cd(ITA)(bimb)_{0.5}(H_2O)_2]_n$ (**6**), have been derived from the designed bifunctional 2-(1-imidazol-yl)terahpthalic acid (H_2ITA) with or without the bis(imidazole) linkers (bib = 1,4-bis(1-imidazol-yl)benzene, bimb = 1,4-bis(imidazol-1-ylmethyl)benzene). X-ray single crystal diffraction analyse reveals that complex **1** and **2** are isomorphic with the same 3D (4,4)–connected $\{4\cdot 6^3\cdot 8^2\}$ net. Complex **3** features a 3D 2–fold interpenetrated (3,4)–connected **fsc** net with the Point symbol of $\{4\cdot 8^2\cdot 10^3\}\{4\cdot 8^2\}$. Complex **4** displays a 2D 3–connected $\{6^3\}$–**hcb** sheet, which can be further expanded into a 3D supramolecular through hydrogen bonding interactions. Complex **5** exhibits an unprecedented 3D 2–fold interpenetrated (3,4)–connected **dmc** net with the Point symbol of $\{4\cdot 8^2\}\{4\cdot 8^5\}$. And complex **6** shows a 3D (3,4)–connected $\{4\cdot 8^2\cdot 10^3\}\{4\cdot 8^2\}$–**fsc** net. Structural comparison reveals that not only the coordination preferences of metal ions but also the auxiliary bis(imidazole) linkers play crucial roles in the control of final structures. Besides, the photoluminescent properties as well as the photocatalytic activities for the degradation of methylene blue (MB) under UV-Vis light of **1**, **3**, **5**, and **6** have been investigated.

Introduction

The assembly of coordination polymers (CPs) have been attracted more and more attentions for their fascinating structures, and various potential chemical, medical and industrial applications acting as zeolite, fluorescence probe, catalyst, drug delivery, molecular switch, and photoelectric sensor and device.[1-3] Although the frontiers of coordination chemistry are focus on buliding functional CPs, the design and assembly of CPs are remian the topics, since the applications are determined by properties, which are essentially determined by structure. [4,5]

Generally speaking, CPs are constructed form organic spacers and inorganic building blocks under suitable situations.[6,7] Many influencing factors, including internal and external factors, have great influences on the structural diversities as well as the properties.[8,9] A myriad of obtained CPs has been proved that the reasonable design of organic linkers is an efficiently route in building CPs.[10,11] The polycarboxylates as well as the N-donors, as two most commonly used organic linkers in the assembly of CPs, have been widely designed and selected for their various coordination modes, and modifiable backbones. It is noteworthy that the polycarboxylates and the N-donors holding different coordination preferences when coordinating with the metal ions for the electron configurations of N and O atoms. However, the bifunctional ligands, which integrated the polycarboxylate and N-donor together, containing both N and O coordinated sites, have more selections in connecting the metal ions. Hitherto, the terephthalic acid (H_2TPA) have been widely used in construction of CPs. When searching the H_2TPA attached the metal ions in the CSD with the help of ConQuest version 1.3, 1878 hits were listed. Besides, the modification of H_2TPA endows the derivatives more selections when coordinating with the metal ions, often leaving interestingly structures. Among them, the 2-position modified H_2TPA derivatives, occupied an important position (Fig. S1, see ESI).[12-14] While the imidazolyl 2-position modified H_2TPA derivatives have been never reported before. Take into consideration of the coordination abilities of imidazole as well as the diverse CPs derived from the similar Py-H_2TPA ligands,[12a,b] we designed a novel bifunctional ligand of 2-(1-imidazol-yl)terahpthalic acid (H_2ITA) and used it to assembly CPs.

Herein, six CPs were reported with the structures ranging from 3D (4,4)–connected $\{4\cdot 6^3\cdot 8^2\}$ net (**1**&**2**), 2-fold 3D interpenetrated (3,4)–connected $\{4\cdot 8^2\cdot 10^3\}\{4\cdot 8^2\}$–**fsc** net (**3**), 2D 3–connected $\{6^3\}$–**hcb** sheet (**4**), 2-fold 3D interpenetrated (3,4)–connected $\{4\cdot 8^2\}\{4\cdot 8^5\}$–**dmc** net (**5**), to 3D (3,4)–connected $\{4\cdot 8^2\cdot 10^3\}\{4\cdot 8^2\}$–**fsc** net (**6**). Luminescent investigations show complexes **1**, **3**, **5**, and **6** are efficient blue emission materials. And they display good photocatalytic activities for the degradation of methylene blue (MB) under UV-Vis light with the efficiency is 67.7 % for **1**, 59.5 % for **3**, 77.2 % for **5**, and 81.5 % for **6** after 5 hours, respectively.

---

[a] *Advanced Material Institute of Research, College of Chemistry and Chemical Engineering, Qilu Normal University, Jinan, 250013, China. E-mail: xiutangzhang@163.com.*
[b] *State Key Laboratory of Crystal Materials, Shandong University , Jinan 250100, China. E-mail: xianzhao@sdu.edu.cn.*

†Electronic Supplementary Information (ESI) available: Powder XRD patterns, TG curves, IR spectra, and X-ray crystallographic data, CCDC-1479965 for **1**, 1479967 for **3**, 1479968 for **4**, 1479969 for **5**, and 1479970 for **6**. See DOI: 10.1039/c6ce00000x.

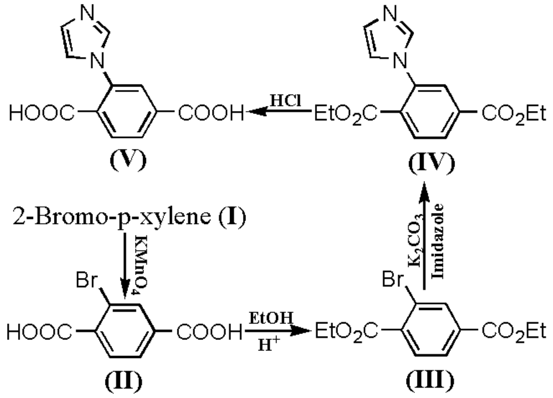

Scheme 1. The synthetic route of H_2ITA.

Experimental Section

Materials and Methods. All chemical reagents were purchased from were purchased from Jinan Henghua Sci. & Tec. Co. Ltd. without further purification**.** IR spectra were measured on a NEXUS 670 FTIR spectrometer in the range of 600-4000 cm^{-1}. Elemental analyses were carried out on a CE instruments EA 1110 elemental analyzer. TGA was measured from 25 to 800 °C on a SDT Q600 instrument at a heating rate 10 °C/min under the N_2 atmosphere (100 mL/min). X-ray powder diffractions were measured on a Panalytical X-Pert pro diffractometer with Cu-Kα radiation. Fluorescence spectra were performed on a Hitachi F-4500 fluorescence spectrophotometer at room temperature. Photocatalytic experiments were evaluated by the degradation of methylene blue (MB) under UV light irradiation using a 300 W metal-halide lamp as the light source. 50 mg powdered catalyst of the obtained complexes was put into 30 min dark adsorption pretreated 50.0 mL 10 mg/L methylene blue (MB) aqueous solution. During the degradation, the reaction solution was sampled at specific time-points and centrifuged to remove the photocatalysts in order to monitor the absorption curves of MB (500-700 nm) by using a Hitachi U-3500 UV-Vis spectrometer.

Design of 2-(imidazol-1-yl)terephthalic acid (H_2ITA) (Scheme 1). ***Synthesis of 2-bromoterephthalic acid (II)***. The mixture of 2-bromo-*p*-xylene (**I**) (0.1 mol, 18.4 g) and 100 mL tert-Butanol in 1000 mL H_2O was refluxed and then potassium permanganate (38 g, 0.24 mol) was slowly added in participle. Refluxed for further 4 h and ethanol was added to remove redundant potassium permanganate. Filtrated solution was acidified with concentrated HCl and white precipice was obtained, which was recrystllized with DMF. The yield is 77%. Anal. (%) calcd. for $C_8H_5BrO_4$: C, 39.21; H, 2.06. Found: C, 39.06; H, 1.97.

Synthesis of diethyl 2-bromoterephthalate (III). 2-bromoterephthalic acid (0.05 mol, 12.2 g) was suspended in 500 mL ethanol with 20 mL H_2SO_4 was refluxed for overnight, and then poured into 1000 mL icewater. The solution was neutralized with ammonium water and extracted with CH_2Cl_2 for three times. Obtained organic solution was concentrated and colourless crystalline product was collected with 90% yield. Anal. (%) calcd. for $C_{12}H_{13}BrO_4$: C, 47.86; H, 4.35. Found: C, 47.70; H, 4.12.

Synthesis of diethyl 2-(imidazol-1-yl)terephthalate (IV). The mixture of III (0.01 mol, 3.0 g), imidazole (0.05 mol, 3.4 g), $CuSO_4$ (0.2 g), and K_2CO_3 (0.05 mol, 6.9 g) was refluxed for 4h and was dissolved in 300 ml EtOH. The solution was decoloured with activated carbon and concentrated to 100 ml. Crude product was obtained and recrystllized with mixed solvent of ethyl acetate and DMF. Anal. (%) calcd. for $C_{15}H_{16}N_2O_4$: C, 62.49; H, 5.59; N, 9.72. Found: C, 62.35; H, 5.46; N, 9.68.

Synthesis of 2-(imidazol-1-yl)terephthalic acid (H_2ITA) (V). The mixture of **IV** (0.01 mol, 2.9 g) and 20 ml concentrated HCl in 100 mL H_2O was refluxed for overnight and filtrated. The obtained precipitate was recrystllized by using DMF to obtained white powder. EI-MS: m/z $[M-H]^-$, 231.05 (calcd for $C_{11}H_8N_2O_4$, 232.05, see Fig. S2). Anal. (%) calcd. for $C_{11}H_8N_2O_4$: C, 56.90; H, 3.47; N, 12.06. Found: C, 56.81; H, 3.38; N, 11.94.

General Syntheses. Six CPs were generally obtained from the hydrothermal reaction of H_2ITA and transition metal salts with or without the help of auxiliary bis(imidazole) linkers. The metal ions as well as the coligands have great influences on the assembly of titled CPs. For **1**−**6**, the IR absorption bands around 3450 cm^{-1} can be attributed to the characteristic peaks of O-H vibrations. The vibrations at about 1400 cm^{-1} and 1610 cm^{-1} correspond to the asymmetric and symmetric stretching vibrations of the carboxyl groups, respectively (Fig. S3).[14]

Synthesis of $\{[M(ITA)]\cdot0.5H_2O\}_n$ (M= Zn for 1, Mn for 2). A mixture of H_2ITA (0.30 mmol, 0.071 g), $ZnSO_4\cdot7H_2O$ (0.30 mmol, 0.086 g), $Na_2MoO_4\cdot2H_2O$ (0.40 mmol, 0.097 g), oxalic acid (0.40 mmol, 0.036g), and 12 mL H_2O was sealed in a 25 mL Teflon-lined stainless steel vessel, which was heated to 130 °C for 5 days and then cooled to room temperature slowly. Colorless block crystals of **1** were obtained. Yield 43 % based on H_2ITA. Anal. (%) calcd. for $C_{22}H_{14}N_4O_9Zn_2$: C, 43.38; H, 2.32; N, 9.20. Found: C, 43.27; H, 2.34; N, 9.17. IR (KBr pellet, cm^{-1}): 3459 (m), 3296 (m), 3020 (m), 1619 (s), 1538 (vs), 1483 (w), 1401 (s), 1361 (s), 1269 (m), 1108 (m), 846 (m), 775 (m). For **2**, the yield is 65 % based on H_2ITA. Anal. (%) calcd. for $C_{22}H_{14}Mn_2N_4O_9$: C, 44.92; H, 2.40; N, 9.52. Found: C, 44.95; H, 2.46; N, 9.47. IR (KBr pellet, cm^{-1}): 3441 (vs), 1617 (s), 1581 (s), 1535 (m), 1483 (m), 1401 (s), 1364 (vs), 1230 (m), 1102 (s), 1026 (m), 954 (m), 847 (s), 806 (m), 773 (s), 733 (m), 654 (m).

Synthesis of $\{[Zn(ITA)(bib)_{0.5}]\cdot1.5H_2O\}_n$ (3). A mixture of H_2ITA (0.20 mmol, 0.047 g), bib (0.30 mmol, 0.063 g), $ZnSO_4\cdot7H_2O$ (0.30 mmol, 0.086 g), NaOH (0.30 mmol, 0.012 g), 12 mL H_2O was sealed in a 25 mL Teflon-lined stainless steel vessel, which was heated to 130 °C for 5 days and then cooled to room temperature slowly. Orange block crystals of **3** were obtained with the yield of 38 % (based on H_2ITA). Anal. (%) calcd. for $C_{32}H_{28}N_{10}O_{11}Zn_2$: C, 44.72; H, 3.28; N, 16.30. Found: C, 44.67; H, 3.33; N, 16.25. IR (KBr pellet, cm^{-1}): 3378 (m), 3145 (s), 1633 (m), 1532 (vs), 1502 (m), 1449 (w), 1331 (m), 1252 (m), 1066 (vs), 963 (m), 946 (m), 835 (m), 752 (m).

Synthesis of $\{[Ni(ITA)(bib)_{0.5}(H_2O)_3]\cdot H_2O\}_n$ (4). The same synthetic procedure as for complex **3** was used except the $ZnSO_4\cdot7H_2O$ was replaced by the $NiCl_2\cdot6H_2O$. Green block crystals of **4** were obtained with the yield of 54 % (based on H_2ITA). Anal. (%) calcd. for $C_{17}H_{19}N_4NiO_8$: C, 43.81; H, 4.11; N, 12.02. Found: C, 43.92; H, 4.15; N, 11.98. IR (KBr pellet, cm^{-1}): 3131 (m), 3069 (m), 1794 (w), 1530 (vs), 1493 (m), 1302 (s), 1259 (m), 1144 (s), 1129 (s), 1110 (s), 1059 (s), 958 (m), 936 (m), 841 (m), 728 (m), 658 (m).

Table 1 Crystal data for **1**, and **3–6**

Complex	**1**	**3**	**4**	**5**	**6**
Empirical formula	$C_{22}H_{14}N_4O_9Zn_2$	$C_{32}H_{28}N_8O_{11}Zn_2$	$C_{17}H_{19}N_4NiO_8$	$C_{36}H_{27}N_8O_9Zn_2$	$C_{18}H_{17}CdN_4O_6$
Formula weight	609.11	855.38	466.07	846.40	497.76
Crystal system	Orthorhombic	Monoclinic	Monoclinic	Monoclinic	Monoclinic
Space group	*Pbcn*	*P*2/*n*	*P*2$_1$/*n*	*P*2/*n*	*C*2/*c*
a (Å)	17.3383(7)	15.2246(8)	7.3222(3)	15.566(3)	29.9762(12)
b (Å)	7.7724(3)	7.3657(4)	25.5967(10)	6.9981(14)	6.7809(3)
c (Å)	15.5015(6)	16.7773(9)	10.3654(4)	17.643(4)	21.3475(9)
α (°)	90	90	90	90	90
β (°)	90	106.831(2)	99.3200(10)	107.99(3)	121.7340(10)
γ (°)	90	90	90	90	90
V(Å^3)	2088.99(14)	1800.81(17)	1917.08(13)	1827.9(6)	3690.5(3)
Z	4	2	4	2	8
D_{calcd} (Mg/m^3)	1.937	1.578	1.615	1.538	1.792
μ(mm^{-1})	2.365	1.404	1.067	1.379	1.229
F(000)	1224	872	964	862	1992
R_{int}	0.1020	0.0811	0.0472	0.0310	0.0574
Final R indices^a	0.0291 (0.0838)	0.0419 (0.1152)	0.0325 (0.0773)	0.0394 (0.1047)	0.0256 (0.0728)
R indices (all data)^a	0.0303 (0.0852)	0.0631 (0.1245)	0.0344 (0.0785)	0.0526 (0.1123)	0.0288 (0.0839)
Gof	1.064	1.030	1.035	1.047	1.067
CCDC number	1479965	1479967	1479968	1479969	1479970

$^aR_1 = \Sigma| |F_o|-|F_c| |/ \Sigma|F_o|$, $wR_2 = [\Sigma w(F_o^2-F_c^2)^2]/ \Sigma w(F_o^2)^2]^{1/2}$

Synthesis of $\{[Zn(ITA)(bimb)_{0.5}]\cdot 0.5H_2O\}_n$ (5). The same synthetic procedure as for complex **3** was used except the bib was replaced by the bimb. Colorless block crystals of **5** were obtained with the yield of 51% (based on H_2ITA). Anal. (%) calcd. for $C_{36}H_{27}N_8O_9Zn_2$: C, 51.08; H, 3.22; N, 13.24. Found: C, 50.97; H, 3.29; N, 13.18. IR (KBr pellet, cm^{-1}): 3584 (m), 3135 (m), 1620 (s), 1521 (m), 1427 (m), 1360 (s), 1243 (m), 1109 (m), 1089 (s), 950 (m), 824 (m), 772 (m), 656 (m).

Synthesis of $[Cd(ITA)(bimb)_{0.5}(H_2O)_2]_n$ (6). The same synthetic procedure as for complex **5** was used except the $ZnSO_4\cdot 7H_2O$ was replaced by the $CdSO_4\cdot 8/3H_2O$. Colorless block crystals of **6** were obtained with the yield of 56 % (based on H_2ITA). Anal. (%) calcd. for $C_{18}H_{17}CdN_4O_6$: C, 43.43; H, 3.44; N, 11.26. Found: C, 43.37; H, 3.41; N, 11.09. IR (KBr pellet, cm^{-1}): 3345 (m), 3149 (m), 1633 (s), 1591 (s), 1553 (s), 1505 (m), 1422 (m), 1395 (s), 1327(s), 1275 (s), 1247 (s), 1096 (s), 1063 (s), 873 (s), 775 (m), 770 (m).

X-ray crystallography. Intensity data collection was carried out on a Siemens SMART diffractometer equipped with a CCD detector using Mo-*Kα* monochromatized radiation (λ = 0.71073 Å) at 296 (2) K. The absorption correction was based on multiple and symmetry-equivalent reflections in the data set using the SADABS program. The structures were solved by direct methods and refined by full-matrix least-squares using the SHELXTL package.[15] All non-hydrogen atoms were refined anisotropically. Hydrogen atoms except those on water molecules were generated geometrically with fixed isotropic thermal parameters, and included in the structure factor calculations. The hydrogen atoms attached to oxygen were refined with O–H=0.85Å and U_{iso}(H) =$1.2U_{eq}$(O). The carboxyl atoms of ITA^{2-} in complex **1** are disordered and were refined with an occupancy ratio of 50:50 for O2A and O2B, respectively. For complex **2**, the obtained crystal data are not ideal to reduce the structure, thus we only give the unit cell parameters (a=17.3409(6) Å, b=7.7719(3) Å, c=15.5112(6) Å, α=90°, β=90°, γ=90°) herein to prove it is an isomorphic structure of complex **1**. And the subsequent characterizations also proved that. Crystallographic data for the CPs are given in Table 1. Selected bond lengths and angles for the CPs are listed in Table S1. For further details on the crystal structure investigations can be obtained from the Cambridge Crystallographic Data Centre, CCDC, 12 Union Road, CAMBRIDGE CB2 1EZ, UK, [Telephone: +44-(0)1223-762-910, Fax: +44-(0)1223-336-033; Email: deposit@ccdc.cam.ac.uk, or by visiting the website of http://www.ccdc.cam.ac.uk/deposit].

Result and Discussion

Structural Description of $\{[M(ITA)]\cdot 0.5H_2O\}_n$ (M= Zn for 1, Mn for 2). Complex **1** and **2** are isomorphic with each other, and complex **1** was selected as a representative to describe herein. Complex **1** crystallizes in the orthorhombic system, space group *Pbcn*. As shown in Fig. 1a, the asymmetric unit consists of one crystallographically independent Zn^{II} ion, one ITA^{2-} ligand, and a half of lattice water molecules. Each Zn^{II} ion located in a distorted $[ZnO_5N]$ octahedral geometry, completed by five oxygen atoms from three different ITA^{2-} ligands, and one nitrogen atom from another ITA^{2-} ligands. Besides, the bond lengths around the centre Zn^{II} ions span in the range of 1.90(8)–2.4328(16) Å.

In the formation of complex **1**, the H_2ITA is completely deprotonated and connected four Zn^{II} ions by adopting μ_4-(η^2:η^1)-κ^1N-(η^2) coordination mode (Mode I, Scheme 2), in which the ω is 40.13(6)° (ω corresponding to the dihedral angle between the rings A and B of the ITA^{2-} ligand). Leaving alone the imidazole group, the chelating+bridging μ_2-η^2:η^1 and the chelating η^2 carboxyl groups of PTA^{2-} linked with Zn^{II} ions, constructed a 2D $[Zn(PTA)]_n$ sheet with the adjancent Zn···Zn distances being 4.008 Å and 10.858 Å (Fig. 1b). And the imidazole groups further expanded those $[Zn(PTA)]_n$ sheets into a 3D framework with the lattice water molecules fulfilled it (Fig. 1c).

From the viewpoint of topology,[16] the final 3D structure can be simplified into an unprecedented (4,4)–connected net with the Point symbol of $\{4\cdot 6^3\cdot 8^2\}$ by denoting the ITA^{2-} ligands as well as the Zn^{II} ions as 4–connected nodes (Fig. 1d). And from the perspective of modular design,[17] the net was built from the tiling of $\{4^2.8g.8h\}+\{6^2.8d.8h\}+\{6^2.8a^2.8d.8g\}$ = $\{4^2.8^2\}+\{6^2.8^2\}+\{6^2.8^4\}$ with the transitivity of 2463 (Fig. 2).

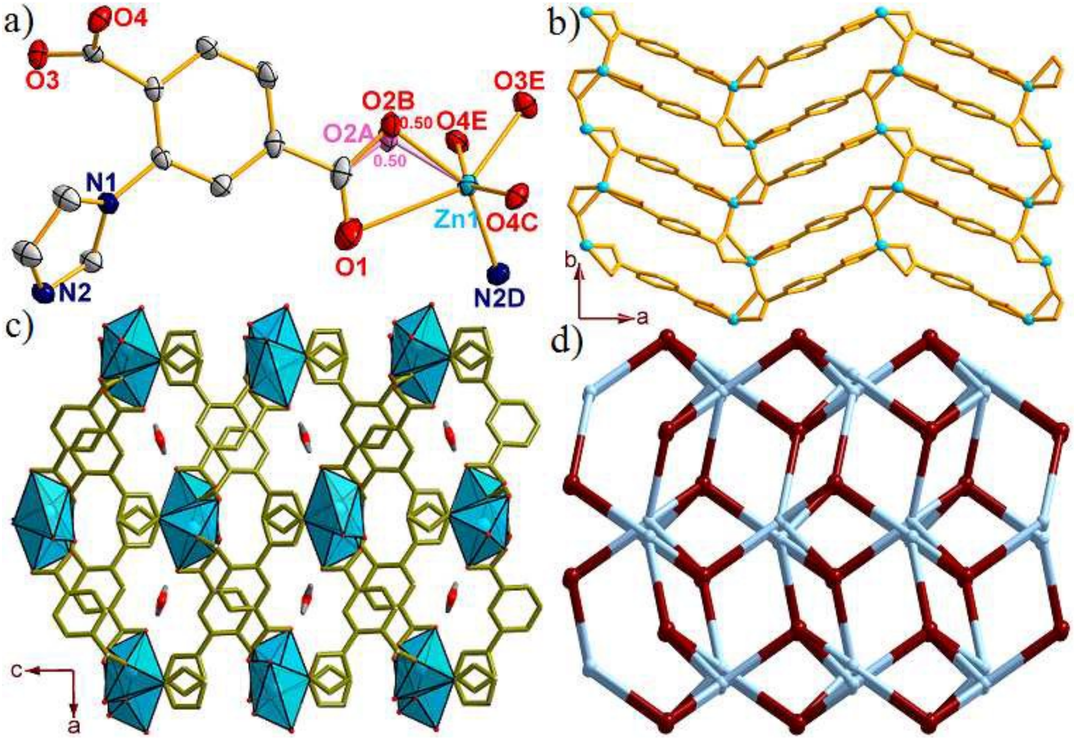

Figure 1. (a) The asymmetric unit of complex **1** with 50% probability ellipsoids. (Symmetry codes: C: 2–*x*, 2–*y*, 1–*z*; D: 1/2+*x*, 1/2+*y*, 1/2–*z*; E: 1/2+*x*, 3/2–*y*, 1–*z*.). (b) The 2D $[Zn(PTA)]_n$ layer view along *c* direction. (c) Schematic view of the 3D framework of **1** along *a* direction. (d) The simplified **3D** (4,4)–connected $\{4{\cdot}6^3{\cdot}8^2\}$ net of **1**.

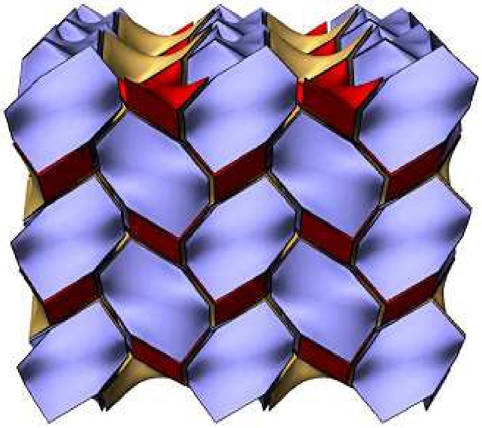

Figure 2. The tiling featured net of complex **1**.

Structural Description of $\{[Zn(ITA)(bib)_{0.5}]{\cdot}1.5H_2O\}_n$ (3). Structural analysis reveals that complex **3** crystallizes in the monoclinic space group *P*2/*n*. The asymmetric unit consists of one Zn^{II} ion, one ITA^{2-}, a half of bib ligands, and one and a half of lattice water molecules (Fig. 3a). The central Zn^{II} ion is tetra-coordinated by two oxygen atoms from two different ITA^{2-} ligands [Zn1–O3C=1.930(3) Å, and Zn1–O2D=1.922(3) Å] and two nitrogen atoms from another two different ITA^{2-} ligand [Zn1–N1=2.038(3) Å]and one bib ligand [Zn1–N3=2.012(3) Å], displaying a distorted $[ZnN_2O_2]$ tetrahedral geometry with the τ_4 parameter being 0.84(2) (τ_4 = [360°–(α+β)]/141°; α and β are the two largest bond angles in the four coordinate complexes.).[18]

Different from complex **1**, the participation of auxiliary bib ligand makes the H_2ITA adopted different coordination mode of μ_3-(η^1)-$\kappa^1 N$-(η^1) coordination mode (Mode II) with ω is 68.52(9)° in the construction of complex **3**. The neighbouring Zn^{II} ions are coupled together by the 3-connected ITA^{2-} ligand, leaving a 2D 3-connected $\{4.8^2\}$-**fes** $[Zn(ITA)]_n$ sheet with the opening area are 5.507×6.783 Å^2, and 10.560×10.876 Å^2, respectively (Fig. 3b). And then the bib linkers bridged the adjacent 2D wave $[Zn(ITA)]_n$ sheets, finally generated into a 3D microporous network with the diameter of the channels is about 16 Å (Fig. 3c). The large channels make the interpenetration possible, thus two independently networks interspersed with each other, finally generating a 2-fold interpenetrated framework (Fig. S4). Calculated by the software of PLATON,[19] the accessible void volume is approximately 12.6 % (226.9 Å^3 out of the 1800.8 Å^3 unit cell volume) after remove the lattice water molecules. The low porosity can mainly attribute to the interpenetration.

Topology analysis reveals that complex **3** is a 3D 2-fold interpenetrated (3,4)-connected **fsc** net with the Point symbol of $\{4{\cdot}8^2{\cdot}10^3\}\{4{\cdot}8^2\}$ by regarding the ITA^{2-} ligand as 3–connected node, and Zn^{II} ion as 4–connected node, respectively (Fig. 3d).

Structural Description of $\{[Ni(ITA)(bib)_{0.5}(H_2O)_3]{\cdot}H_2O\}_n$ (4). Complex **4** crystallizes in the monoclinic system *P*2$_1$/*n*. As shown in Fig. 4a, there are one Ni^{II} ion, one ITA^{2-} ligand, a half of bib ligands, three coordinated water molecules, and one lattice water molecule in the asymmetric unit. Each Ni^{II} ion is octa–coordinated by four oxygen atoms from one ITA^{2-} ligand and three coordinated water molecules, two N atoms from one ITA^{2-} ligand and one bib ligand, leaving the distorted octahedral coordination geometry. And the Ni–O/N bond lengths are in the range of 2.0382(17)–2.1228(18) Å.

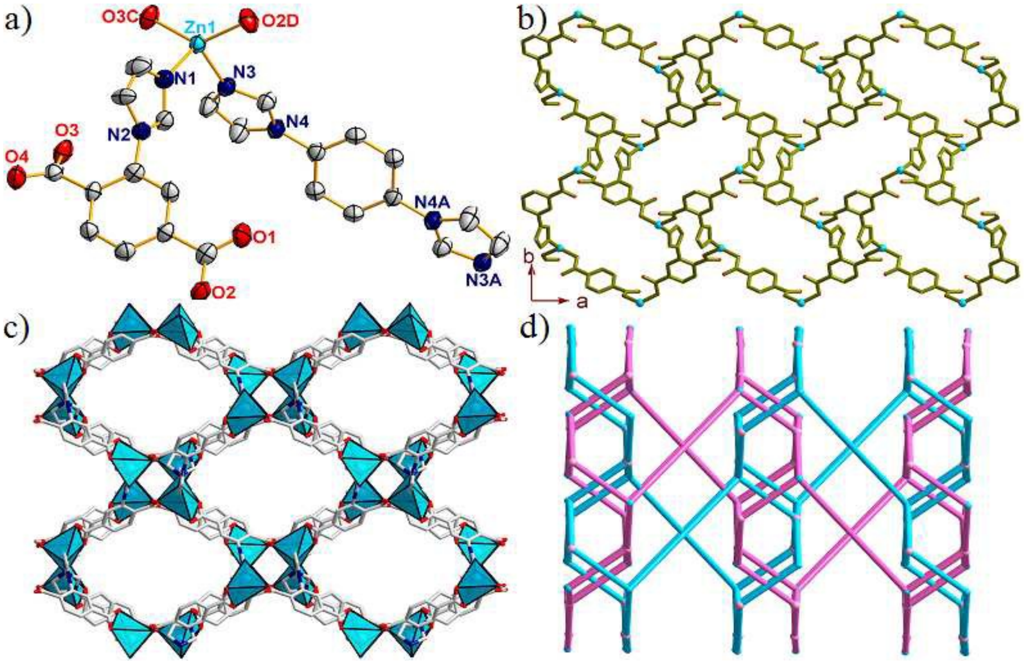

Figure 3. (a) The asymmetric unit of complex **3** with 50% probability ellipsoids. (Symmetry codes: A: 1–*x*, 1–*y*, 1–*z*; C: 2–*x*, 2–*y*, 1–*z*; D: 3/2–*x*, 1+*y*, 1/2–*z*.). (b) The 2D $[Zn(ITA)]_n$ layer view along *c* direction. (c) Schematic view of the 3D framework of **3**. (d) The 2-fold (3,4)-connected $\{4 \cdot 8^2 \cdot 10^3\}\{4 \cdot 8^2\}$–**fsc** net of **3**.

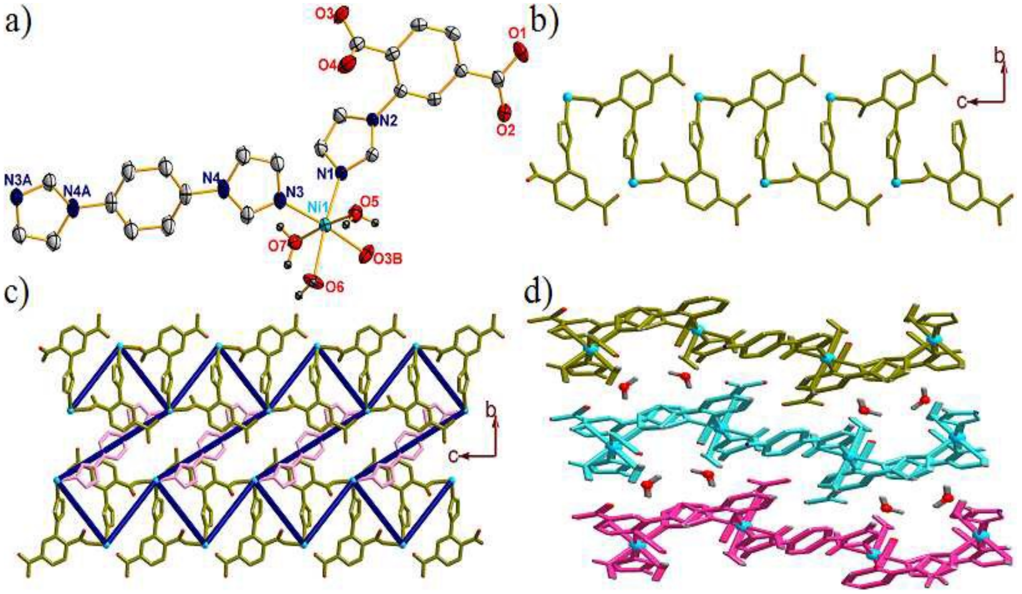

Figure 4. (a) The asymmetric unit of complex **4** with 50% probability ellipsoids. (Symmetry codes: A: 1–*x*, 2–*y*, 2–*z*; B: –1/2+*x*, 3/2–*y*, –1/2+*z*.). (b) The 1D $[Zn(ITA)]_n$ chain along *a* direction. (c) Schematic view of the 2D $\{6^3\}$–**hcb** sheet of **4** along *a* direction. (d) The 3D packing supramolecular structure of **4**.

In the formation of complex **4**, although the H_2ITA is also completely deprotonated, rather than participate in the coordination geometry of central metal ion, one carboxyl group act as the charge balancing. The ITA^{2-} ligand displays μ_2-(η^1)-$\kappa^1 N$ coordination mode (Mode III) with ω is 59.55(8)°, linking two Ni^{II} ions, resulting to a 1D $[Ni(ITA)]_n$ snake-like chain with the Ni···Ni distance being 8.450(8) Å along *a* axis (Fig. 4b). Those 1D $[Ni(ITA)]_n$ chains are further expanded into a 2D $\{6^3\}$–**hcb** sheet (Fig. S5) with the bib separated Ni···Ni distance is 13.690(7) Å (Fig. 4c). Those sheets interacted with the lattice water molecules through the O–H···O hydrogen bonding interactions (Table 2), finally constructed a 3D supramolecular structure (Fig. 4d and Fig. S6).

Table 2. The hydrogen bonds in complex **4**.

D−H···A	d(H···A)/ Å	d(D···A)/ Å	∠(D−H···A)/ °
O(5)-H(1W)-O(4)$^{\#1}$	1.87	2.67	162
O(5)-H(2W)-O(2)$^{\#2}$	1.99	2.79	164
O(6)-H(3W)-O(2)$^{\#2}$	2.06	2.82	155
O(6)-H(4W)-O(1)$^{\#3}$	1.90	2.69	160
O(7)-H(5W)-O(2)$^{\#2}$	1.93	2.75	177
O(7)-H(6W)-O(1)$^{\#3}$	1.99	2.80	168
O(8)-H(8W)-O(3)$^{\#4}$	2.05	3.08	124

Symmetry codes: #1: *x*−1/2, −*y*+3/2, *z*−1/2; #2: *x*+1/2, −*y*+3/2, *z*+1/2; #3: −*x*+1/2, *y*+1/2, −*z*+1/2; #4: *x*−1, *y*, *z*.

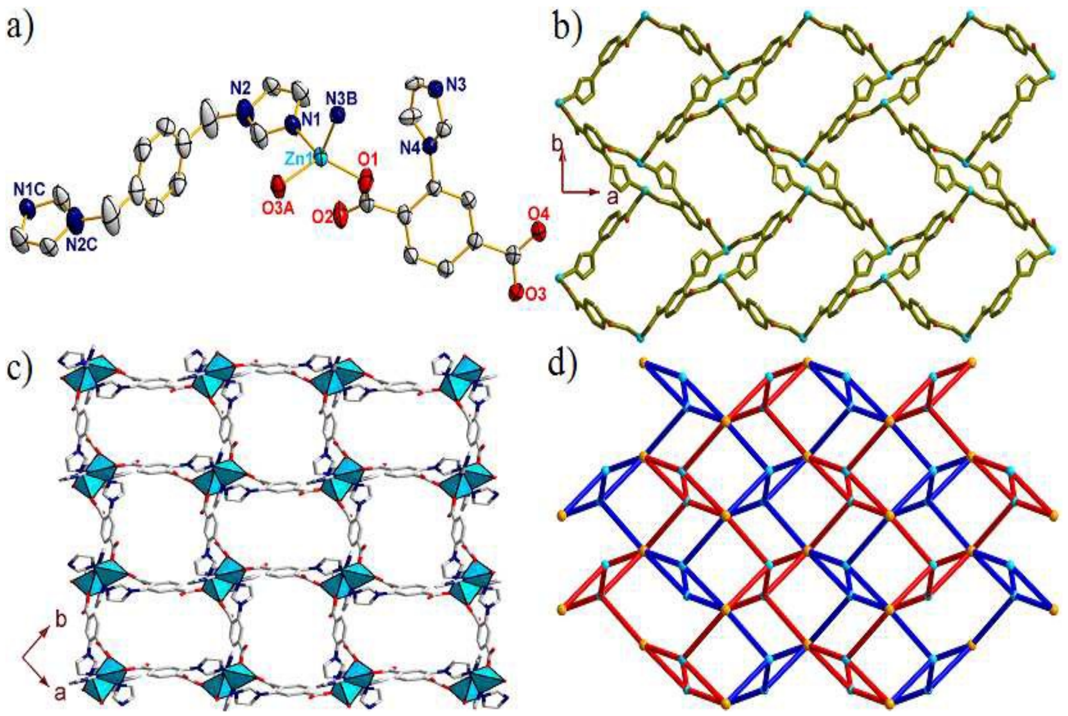

Figure 5. (a) The asymmetric unit of complex **5** with 50% probability ellipsoids. (Symmetry codes: A: –1/2+*x*, –*y*, –1/2+*z*; B: 1–*x*, 1–*y*, 1–*z*; C: 1–*x*, 1–*y*, –*z*.). (b) The 2D [Zn(ITA)]$_n$ sheet of complex **5** along *c* direction. (c) The 3D framework of **5** along *c* direction. (d) The 2-fold (3,4)-connected $\{4{\cdot}8^2\}\{4{\cdot}8^5\}$–**dmc** net of **5**.

Structural Description of {[Zn(ITA)(bimb)$_{0.5}$]·0.5H$_2$O}$_n$ (5). X-ray single-crystal analysis reveals that complex **5** crystallizes in monoclinic system, *P*2/*n* space group and the asymmetric unit consists of one Zn^{II} ion, one ITA^{2-} ligand, a half of bimb ligand lying about independent inversion centre, and a half of lattice water molecules. As can be seen in the Fig. 5a, the Zn^{II} ion is surrounded by two oxygen atoms from two different ITA^{2-} ligands, and two nitrogen atoms from one ITA^{2-} ligand and one bimb ligand, exhibiting a distorted tetrahedral coordination geometry (τ_4 = 0.83(4)). The Zn─O/N bond lengthes are in the range of 1.917(6)─2.025(6) Å.

In the assembly of complex **5**, the H$_2$ITA ligand adopted the same coordination mode of μ_3-(η^1)-κ^1*N*-(η^1) (Mode II) with that in complex **3**, connecting three Zn^{II} ions *via* pyridine N atom and two monodentate carboxyl groups, finally generated a 2D [Zn(ITA)]$_n$ sheet with the opening area being 5.509×6.738 Å^2, and 10.517×10.895 Å^2, respectively (Fig. 5b). And the dihedral angle of ω is 65.59(8)°, indicating the bib ligand in complex **3** and the bimb ligand in complex **5** displaying similar coordination synergistic effect. The bimb ligands linked with the adjacent 2D [Zn(ITA)]$_n$ layers, successfully constructed a 3D microporous framework with rectangle opening is 10.895×10.517 Å^2 (Fig. 5c). Similar with complex **3**, the large channels also bring interpenetration. Two frameworks interpenetrated with each other, emerging a 2-fold interpenetrated framework. The calculated total potential solvent accessible volume for complex **5** calculated by the free PLATON software, upon removal of guest solvent molecules, was estimated to be 7.4 % (135.2 Å^3/1827.9 Å^3). Low porosity can be owed to the interpenetration.

Topologically speaking, the final structure of complex **5** can be described as a 3D 2-fold interpenetrated (3,4)-connected **dmc** net with the Point symbol of $\{4{\cdot}8^2\}\{4{\cdot}8^5\}$ by regarding the ITA^{2-} ligand as 3–connected node, and Zn^{II} ion as 4–connected node, respectively (Fig. 5d).

Structural Description of [Cd(ITA)(bimb)$_{0.5}$(H$_2$O)$_2$]$_n$ (6). Structural analysis reveals that complex **6** crystallizes in the monoclinic system, *C*2/*c* space group. There are one Cd^{II} ion, one ITA^{2-} ligand, a half of bimb ligands, and two coordinated water molecules in the asymmetric unit. As shown in Fig. 6a, the Cd^{II} ion located in a distorted [CdO$_5$N$_2$] pentagonal bipyramid coordination geometry, completed by five oxygen atoms form two ITA^{2-} ligands [Cd1–O4=2.483(2) Å, Cd1–O1C=2.510(2) Å, and Cd1–O2C=2.438(2) Å] and two coordinated water molecules [Cd1–O5=2.417(2) Å, and Cd1–O6=2.497(2) Å], and two nitrogen atoms from one ITA^{2-} ligand [Cd1–N1B=2.233(2) Å] and one bimb ligand [Cd1–N3=2.245(2) Å].

The large atomic radius of Cd^{II} ion makes the deprotonated ITA^{2-} ligand adopting μ_3-(η^2)-κ^1*N*-(η^1) coordination mode (Mode IV) with the ω is 53.99(3)°. And the 3-connected ITA^{2-} ligand linked the Cd^{II} ions, forming a 2D [Cd(ITA)]$_n$ sheet with two squares with the area being 5.688×6.989 Å^2, and 10.770×11.017 Å^2, respectively (Fig. 6b). And the bimb act as the bridging linkers, hinged the neighbouring 2D [Cd(ITA)]$_n$ sheets together into a 3D framework, in which the bimb separated Cd···Cd distance is 14.652(2) Å (Fig. 6c).

Topology analysis reveals that complex **6** is a 3D framework with (3,4)–connected $\{4{\cdot}8^2{\cdot}10^3\}\{4{\cdot}8^2\}$–**fsc** net by simplifying ITA^{2-} ligands as 3–connected nodes, and Cd^{II} ions as 4–connected nodes, respectively (Fig. 6d). It is noteworthy that although complexes **3** and **5** are both **fsc** net, they hold different folds, with two-fold for **3**, and single for **5**, which can be mainly attributed to the length of ancillary bis(imidazole) linkers as each metal ion linked similar organic ligands (three ITA^{2-} ligands and one ancillary bis(imidazole) linkers) in two complexes.

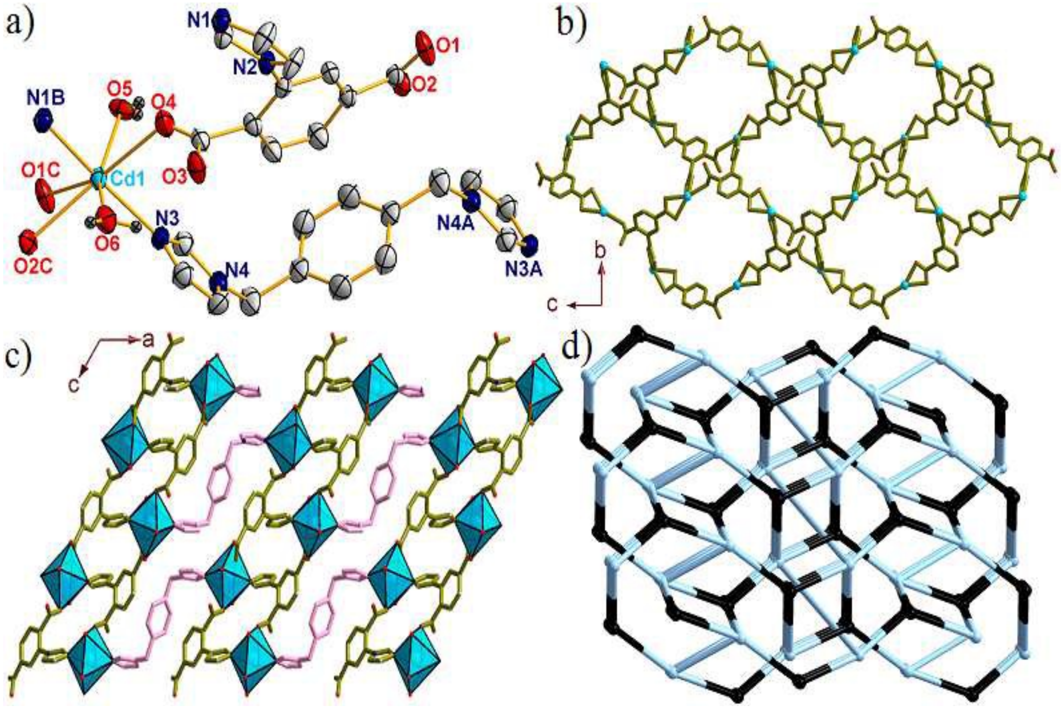

Figure 6. (a) The asymmetric unit of complex **6** with 50% probability ellipsoids. (Symmetry codes: A: 3/2–*x*, 1/2–*y*, 2–*z*; B: 2–*x*, 2–*y*, 2–*z*; C: *x*, 1–*y*, –1/2+*z*.). (b) The 2D $[Cd(ITA)]_n$ sheet in complex **6** along *a* direction. (c) The 3D framework of complex 6 along *b* direction. (d) The simplified 3D (3,4)–connected $\{4{\cdot}8^2{\cdot}10^3\}\{4{\cdot}8^2\}$–**fsc** net for **6**.

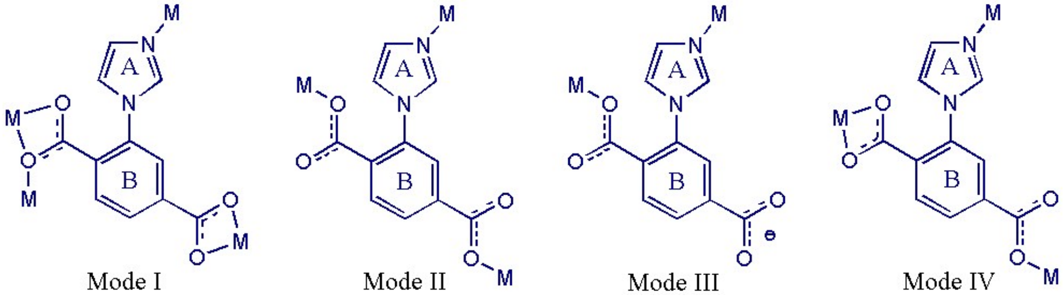

Scheme 2. The diverse coordination modes of H_2ITA.

Table 3 The detailed comparisons of complexes **1**, and **3**–**6**.

	Coord. Modes	Dihedral angle ω (°) ^{a}	M-ITA motifs	Structure	Point symbol
1	Mode I	40.13(6)	3D $[Zn(ITA)]_n$ net	3D (4,4)–connected net	$\{4{\cdot}6^3{\cdot}8^2\}$
3	Mode II	68.52(9)	2D $[Zn(ITA)]_n$ sheet	3D 2-fold interpenetrated (3,4)-connected **fsc** net	$\{4{\cdot}8^2{\cdot}10^3\}\{4{\cdot}8^2\}$
4	Mode III	59.55(8)	1D $[Ni(ITA)]_n$ chain	2D 3-connected **hcb** sheet	$\{6^3\}$
5	Mode II	65.59(8)	2D $[Zn(ITA)]_n$ sheet	3D 2-fold interpenetrated (3,4)–connected **dmc** net	$\{4{\cdot}8^2\}\{4{\cdot}8^5\}$
6	Mode IV	53.99(3)	2D $[Cd(ITA)]_n$ sheet	3D (3,4)–connected **fsc** net	$\{4{\cdot}8^2{\cdot}10^3\}\{4{\cdot}8^2\}$

^{a} ω is the dihedral angle between the rings A and B of the ITA^{2-} ligands.

Structural Comparison. As shown in Scheme 2 and Table 3, in complex **1**, and **3–6**, the H_2ITA are completely deproponated and coordinated with the metal ions through the monodentate η^1, chelating η^2, and chelating+bridging μ_2-η^2:η^1 carboxyl groups, as well as the imidazole groups. Although the coordination modes are similar, the obtained $[M(ITA)]_n$ motifs are distinct from 1D $[Ni(ITA)]_n$ chain to 3D $[Zn(ITA)]_n$ net, which can be mainly attributed to dihedral angles (ω) between the imidazole ring and the phenyl ring and the coordination preferences of metal ions: i) the Zn^{II} ions tend to adopted tetrahedral geometry in complex **3** and **5**, the Ni^{II} ion located in distorted octahedral coordination geometry in complex **4**, while the Cd^{II} ion is surrounded by seven N/O atoms, leaving a pentagonal bipyramid geometry in complex **6**; ii) the dihedral angles (ω) indicating the ITA^{2-} ligands are twisted with various angles in titled complexes and can expanded into different directions. The comparisons among the final packing structures suggested that the bridging imidazole linkers play important roles in the assembly of titled complexes, act as bridgers joining neighboring $[M(ITA)]_n$ motifs, finally leaving 2D sheets, 3D nets, and the 3D interpenetrated nets.

For complex **1** and **2**, when the Na_2MoO_4 was not added as starting reacting materials, only the unknown yellow powders were obtained. Thus we think the Na_2MoO_4 act as a additive agent and the oxalic acid incorporating with NaOH provding a buffer system. With the imidazole linkers were introduced, two 3D interpenetrated nets were obtained, with 2-fold (3,4)-connected **fsc** net for **3**, and 2-fold (3,4)–connected **dmc** net for **5**, respectively, which indicating the lengths of bis(imidazole) linkers greatly impact the frameworks as well as the final structures. And the comparisons between **3**/**4** and **5**/**6** demonstrated that the preferences of different metal ions make the obtained architectures diverse. Overall, by adjusting the reaction conditions, six CPs were obtained with the structures ranged from 2D 3–connected 6^3-**hcb** net (**4**), 3D (4,4)–connected $\{4{\cdot}6^3{\cdot}8^2\}$ net (**1** & **2**), 3D (3,4)–connected $\{4{\cdot}8^2{\cdot}10^3\}\{4{\cdot}8^2\}$-**fsc** net (**6**), 2-fold 3D (3,4)–connected $\{4{\cdot}8^2{\cdot}10^3\}\{4{\cdot}8^2\}$-**fsc** net (**3**), to 2-fold 3D (3,4)–connected $\{4{\cdot}8^2\}\{4{\cdot}8^5\}$-**dmc** net (**5**).

X-ray Power Diffraction Analyses and Thermal Analyses. The samples of those CPs were prepared according to the synthesis section, and then were washed with the mixed solvent of water/ethanol. After naturally drying step, the obtained crystals were carefully handpicked and collected to check the phase purity. As shown in Fig. S7, the experimental PXRD patterns are in agreement with the simulated ones, demonstrating the good phase purity of the complexes. The experiments of thermogravimetric analysis (TGA) were performed on samples of **1**-**6** under N_2 atmosphere with a heating rate of 10 °C min^{-1}, shown in Fig. S8. For **1**, the preliminary weight loss below 115 ^oC corresponds to the release of coordinated water molecules (obsd: 3.01%; calcd: 2.95%) and then the framework can existed stable until the temperature up to 345 °C. For **2**, the first weight loss in the temperature range of 50-110 °C can be attributed to the release of coordinated and lattice water molecules (obsd: 3.13%; calcd: 3.06%). No obvious weight loss is observed until the decomposition of the framework occurs at 365 °C. For **3**, the TGA curve shows a weight loss about 6.97% below 120 °C, which can be ascribed to the release of lattice water molecules (6.42%). And then the residual frameworks exist stably below 300 ^oC. Above this temperature, the net collapsed with the organic linkers released. In the case of **4**, the weight loss of 8.83 % within the temperature range of 30-210 °C, is ascibed to the release of both the coordinated and lattice water molecules (calc. 9.05 %), and then no further weight loss before the decomposition at 335°C. For **5**, the lattice water molecules loss around 100°C, with the weight loss of 2.37 % (calc. 2.13 %). And then the organic pillars of the frameworks begin to pyrolyze when the temperature up to 360 °C. For **6**, the structure can be stable up to 105 °C, with a total weight loss of a 7.65% in the temperature range of 105−175 °C, corresponding to two lattice water molecules (calc. 7.23 %). Then the framework followed by a plateau of stability until 340 °C.

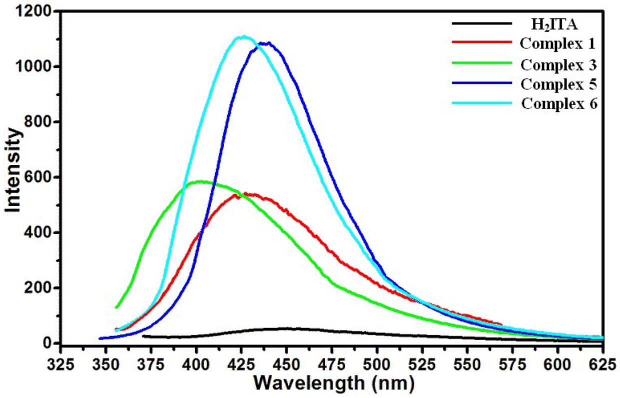

Figure 7. Emission spectra of the free H_2ITA ligand and complexes **1**, **3**, **5**, and **6** in the solid state at room temperature.

Photoluminescent Properties. The fluorescence spectrum of the free H_2ITA ligand, complexes **1**, **3**, **5**, and **6** were examined in the solid state at room temperature, shown in Fig. 7. The free ligand of H_2ITA shows violet fluorescent emission band at 450 nm under 350 nm wavelength excitation, which is attributed to the $\pi^*\rightarrow n$ or $\pi^*\rightarrow\pi$ transitions.[20] For complexes **1**, **3**, **5**, and **6**, the emission spectra exhibit strong blue-fluorescent emission peaks at 427 nm (λ_{ex} = 335 nm) for **1**, 402 nm (λ_{ex} = 335 nm) for **3**, 438 nm (λ_{ex} = 326 nm) for **5**, and 425 nm (λ_{ex} = 335 nm) for **6**, respectively. The blue shift of those coordination complexes can be assigned to strong electrostatic interaction between metal ions and the organic ligands by inserting the lone pair electrons of N/O atoms into the empty orbits of the metal ions.[21] The emission is neither metal-to-ligand charge transfer (MLCT) nor ligand-to-metal transfer (LMCT) in nature since the Zn^{II} and Cd^{II} ions are difficult to oxidize or reduce due to its d^{10} configuration.[22,23] Thus, they can be assigned to intraligand ($\pi^*\rightarrow n$ or $\pi^*\rightarrow\pi$) emission. The higher PL intensities of CPs can be attributed to the increasing of the conjugated system when the metal ions coordinating with the organic ligands. The incorporation of metal ions and organic ligands effectively increases the conformational rigidity of the ligand and reduces the loss of energy *via* vibration motions.[24] As illustrated by the CIE chromaticity coordinates of the emission spectra in Fig. S6, the overall emission is located in the blue region with CIE chromaticity coordinate of (0.15, 0.13) for **1**, (0.15, 0.10) for **3**, (0.15, 0.08) for **5**, and (0.15, 0.08) for **6**, respctively (Fig. S9).[25] The observation indicates that the polymeric complexes of **1**, **3**, **5**, and **6** may be excellent candidate for the efficient photocatalytic materials. And the quantum yields of complexes **1**, **3**, **5**, and **6** are 3.4%, 4.1%, 3.7%, and 4.0%, respectively.

Photocatalytic Activities. Many coordination architectures have been used as the photocatalysts in the degradation of organic dyes, and the luminescent investigations also show the four Zn^{II}/Cd^{II} CPs holding strong intensities in the blue region. Those mentioned points inspired us to evaluate the photocatalytic activities of those complexes in the purification of Methylene blue (MB). The decomposition of dye methylene blue (MB) was monitored by the characteristic absorption band at 664 nm. As illustrated in Fig. 8-11, changes in the concentration of MB solution were plotted versus irradiation time. The calculation results show that the degradation efficiency of MB is up to 67.7 % for **1**, 59.5 % for **3**, 77.2 % for **5**, and 81.5 % for **6** after 5 hours, respectively. Under the same conditions, the total catalytic degradation efficiency of the control experiment under illumination after 5 hours is 44.1 % (Fig. S10). The photocatalystic investigation shows complex **5** and **6** exhibiting relatively good photocatalytic activity than complex **1** and **3** for dye methylene blue (MB) degradation in aqueous solution under UV light, which may be attributed to the intensity of emission. The possible mechanism for the MB degradation is proposed as described in the previous literature.[26] Under the irradiation of UV-Vis light, the organic ligands were induces to produce O or N-metal charge transfer promoting electrons from the highest occupied molecular orbital (HOMO) to the lowest unoccupied molecular orbital (LUMO). Therefore, the HOMO strongly needs one electron to return to its stable state. Thus, one electron was captured from water molecules, which was oxygenated to generate the ·OH radicals. And then the ·OH active species could decompose the MB effectively to complete the photocatalytic process. In order to investigate the reusable performance of those complexes, we repeated the degradation of organic dyes three times and glad to find they keep similar photocatalytic efficiencies (Fig. S11-S14).

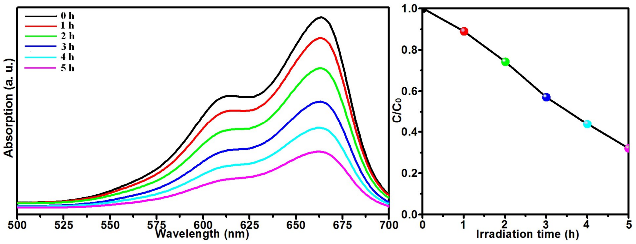

Figure 8. UV-Vis absorption spectra of the MB solutions degraded by complex **1** as photocatalyst under UV irradiation at different time intervals.

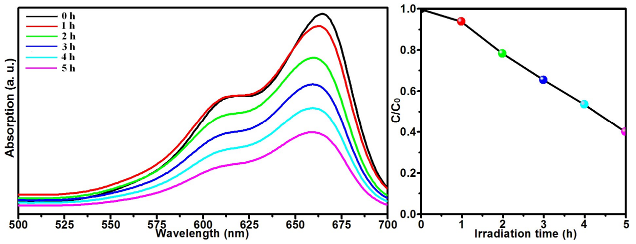

Figure 9. UV-Vis absorption spectra of the MB solutions degraded by complex **3** as photocatalyst under UV irradiation at different time intervals.

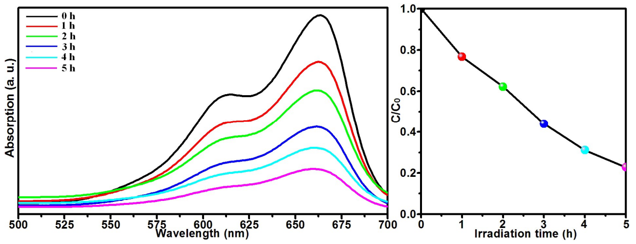

Figure 10. UV-Vis absorption spectra of the MB solutions degraded by complex **5** as photocatalyst under UV irradiation at different time intervals.

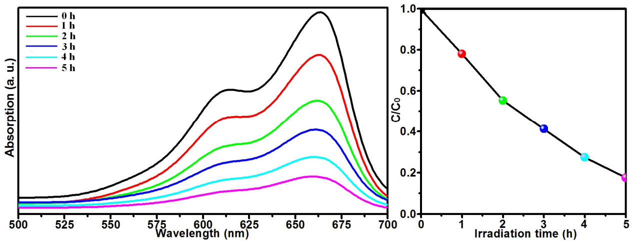

Figure 11. UV-Vis absorption spectra of the MB solutions degraded by complex **6** as photocatalyst under UV irradiation at different time intervals.

Conclusions

In summary, based on the designed bifunctional H_2ITA ligand, six CPs were obtained, with the structures ranging from 3D (4,4)–connected $\{4{\cdot}6^3{\cdot}8^2\}$ net (**1&2**), 2-fold 3D interpenetrated (3,4)–connected $\{4{\cdot}8^2{\cdot}10^3\}\{4{\cdot}8^2\}$–**fsc** net (**3**), 2D 3–connected $\{6^3\}$–**hcb** sheet (**4**), 2-fold 3D interpenetrated (3,4)–connected $\{4{\cdot}8^2\}\{4{\cdot}8^5\}$–**dmc** net (**5**), to 3D (3,4)–connected $\{4{\cdot}8^2{\cdot}10^3\}\{4{\cdot}8^2\}$–**fsc** net (**6**). Luminescent investigations indicate that complexes **1**, **3**, **5**, and **6** are efficient blue emission materials. And they show good photocatalytic activities for the degradation of methylene blue (MB) under UV-Vis light with the efficiency is 67.7 % for **1**, 59.5 % for **3**, 77.2 % for **5**, and 81.5 % for **6** after 5 hours, respectively.

Acknowledgements. This work was supported by financial support from the National Natural Science Foundation of China (Grant No. 21451001) and the Key Discipline, Innovation Team, and Key Lab. of Qilu Normal University.

Notes

The authors declare no competing financial interest.

References

1. (a) A. Dhakshinamoorthy, A. M. Asiri and H. Garcia, *Chem. Soc. Rev.*, 2015, **44**, 1922; (b) T. R. Cook, Y. R. Zheng and P. J. Stang, *J. Chem. Rev.*, 2013, **113**, 734; (c) D. S. Li, Y. P. Wu, J. Zhao, J. Zhang and J. Y. Lu, *Coord. Chem. Rev.*, 2014, **261**, 1; (d) G. Férey and C. Serre, *Chem. Soc. Rev.*, 2009, **38**, 1380; (e) A. Mallick, B. Garai, M. A. Addicoat, P. S. Petkov, T. Heine and R. Banerjee, *Chem. Sci.*, 2015, **6**, 1420; (f) X. Yang and D. Yan, *Chem. Sci.*, 2016, **7**, 4519.
2. (a) D. B. Shinde, S. Kandambeth, P. Pachfule, R. R.Kumar and R. Banerjee, *Chem. Commun.*, 2015, **51**, 310; (b) E. D. Bloch, W. L. Queen, R. Krishna, J. M. Zadrozny, C. M. Brown and J. R. Long, *Science*, 2012, **335**, 1606; (c) A. Goeppert, M. Czaun, J. Jones, G. K. S. Prakash and G. A. Olah, *Chem. Soc. Rev.*, 2014, **43**, 7995; (d) D. –X. Zhang, H. –X. Zhang, T. Wen, D. –S. Li and J. Zhang, *Inorg. Chem. Front.*, 2016, **3**, 263; (e) X. Yang and D. Yan, *Adv. Opt. Mater.*, 2016, **4**, 897; (f) T. Panda, K. M. Gupta, J. Jiang and R. Banerjee, *CrystEngComm*, 2014, **16**, 4677.
3. (a) V. Guillerm, D. Kim, J. F. Eubank, R. Luebke, X. Liu, K. Adil, M. S. Lah and M. Eddaoudi, *Chem. Soc. Rev.*, 2014, **43**, 6141; (b) J. B. Lin, W. Xue, B. Y. Wang, J. Tao, W. X. Zhang, J. P. Zhang and X. M. Chen, *Inorg. Chem.*, 2012, **51**, 9423; (c) X. Zhang, L. Fan, W. Zhang, Y. Ding, W. Fan and X. Zhao, *Dalton Trans.*, 2013, **42**, 16562; (d) Q. Zhang, H. Zhang, S. Zeng, D. Sun and C. Zhang, *Chem-Asian J.*, 2013, **8**, 1985; (e) U. P. Singh, S. Narang, P. Pachfule and R. Banerjee, *CrystEngComm*, 2014, **16**, 5012; (f) Y. Tang, W. He, Y. Lu, J. Fielden, X. Xiang and D. Yan, *J. Phys. Chem. C*, 2014, 118, 25365.
4. (a) W. L. Leong and J. J.Vittal, *Chem. Rev.*, 2011, **111**, 688; (b) A. Schneemann, V. Bon, I. Schwedler, I. Senkovska, S. Kaskel and R. A. Fischer, *Chem. Soc. Rev.*, 2014, **43**, 6062; (c) X. H. Chang, Y. Zhao, M. L. Han, L. F. Ma and L. Y. Wang, *CrystEngComm*, 2014, **16**, 6417; (d) W. Shi, S. Song and H. Zhang, *Chem. Soc. Rev.*, 2013, **42**, 5714; (e) D. Yan, Y. Tang, H. Lin and D. Wang, *Sci. Rep.*, 2014, **4**, 4337; (f) G. Fan, X. Yang, R. Liang, J. Zhao, S. Li and D. Yan, *CrystEngComm*, 2016, **18**, 240.
5. (a) P. Pachfule, S. Kandambeth, D. D. Díaz and R. Banerjee, *Chem. Commun.*, 2014, **50**, 3169; (b) U. J. Williams, B. D. Mahoney, A. J. Lewis, P. T. DeGregorio, P. J. Carroll and E. J. Schelter, *Inorg. Chem.*, 2013, **52**, 4142; (c) M. L. Han, X. C. Chang, X. Feng, L. F. Ma and L. Y. Wang, *CrystEngComm*, 2014, **16**, 1687; (d) K. Su, F. Jiang, J. Qian, L. Chen, J. Pang, S. M. Bawaked, M. Mokhtar, S. A. Al-Thabaiti and M. Hong, *Inorg. Chem.,* 2015, **54**, 3183; (e) L. Fan, Y. Gao, G. Liu, W. Fan, W. Song, L. Sun, X. Zhao and X. Zhang, *CrystEngComm*, 2014, **16**, 7649; (f) J. –Q. Sha, L. –J. Sun, P. –P. Zhu and J. Jiang, *CrystEngComm*, 2016, **18**, 283.
6. (a) A. Aijaz, J. -K. Sun, P. Pachfule, T. Uchida and Q. Xu, *Chem. Commun.*, 2015, **51**, 13945; (b) L. Fan, X. Zhang, D. Li, D. Sun, W. Zhang and J. Dou, *CrystEngComm*, 2013, **15**, 349; (c) L. P. Xue, C. X. Chang, S. H. Li, L. F. Ma and L. Y. Wang, *Dalton Trans.,* 2014, **43**, 7219; (d) L. L. Liu, C. X. Yu, J. Sun, P. P. Meng, F. J. Ma, J. M. Du and L. F. Ma, *Dalton Trans.,* 2014, **43**, 2915; (e) L. L. Liu, C. X. Yu, Y. R. Li, J. J. Han, F. J. Ma and L. F. Ma, *CrystEngComm*,

2015, **17**, 653; (f) W. Yan, N. Hao and H. Zheng, *Dalton Trans.*, 2016, **45**, 6418.

7. (a) S. Dutta, D. -K. Bučar, E. Elacqua and L. R. MacGillivray, *Chem. Commun.*, 2013, **49**, 1064; (b) X. Zhang, L. Fan, W. Zhang, W. Fan, L. Sun and X. Zhao, *CrystEngComm*, 2014, **16**, 3203; (c) L. Zhang, Y. Zhang, R. Wang, Z. Kang, X. Liu, D. Sun and Q. Meng, *CrystEngComm*, 2015, **17**, 6591; (d) X. Zhang, L. Fan, Z. Sun, W. Zhang, W. Fan, L. Sun and X. Zhao, *CrystEngComm*, 2013, **15**, 4910; (e) L. Fan, X. Zhang, W. Zhang, Y. Ding, W. Fan, L. Sun, Y. Pang and X. Zhao, *Dalton Trans.*, 2014, **43**, 6701; (f) T. Wang, C. Zhang, Z. Ju and H. Zheng, *Dalton Trans.*, 2015, **44**, 6926.
8. (a) R. E. Osta, M. Frigoli, J. Marrot, N. Guillou, H. Chevreau, R. I. Walton and F. Millange, *Chem. Comm.*, 2012, **48**, 10639; (b) J. Zhao, D. S. Li, X. J. Ke, B. Liu, K. Zou and H. M. Hu, *Dalton Trans.,* 2012, **41**, 2560; (c) L. Fan, X. Zhang, W. Zhang, Y. Ding, W. Fan, L. Sun and X. Zhao, *CrystEngComm*, 2014, **16**, 2144; (d) M. Yan, F. Jiang, Q. Chen, Y. Zhou, R. Feng, K. Xiong and C. Hong, *CrystEngComm*, 2011, **13**, 3971; (e) J. –C. Li, H. –X. Li, H. –Y. Li, W. –J. Gong and J. –P. Lang, *Cryst. Growth Des.*, 2016, **16**, 1617; (f) L. Fan, W. Fan, B. Li, X. Liu, X. Zhao and X. Zhang, *Dalton Trans.*, 2015, **44**, 2380.
9. (a) X. Lin, J. Jia, X. Zhao, K. M. Thomas, A. J. Blake, G. S. Walker, N. R. Champness, P. Hubberstey and M. Schrder, *Angew. Chem. Int. Ed.*, 2006, **45**, 7358; (b) F. Meng, M. Zhang, K. Shen, Y. Li and H. Zheng, *Dalton Trans.*, 2015, **44**, 1412; (c) H. R. Fu, F. Wang and J. Zhang, *Dalton Trans.,* 2014, **43**, 4668; (d) T. Panda, P. Pachfule and R. Banerjee, *Chem. Commun.*, 2011, **47**, 7674; (e) L. Fan, W. Fan, W. Song, L. Sun, X. Zhao and X. Zhang, *Dalton Trans.*, 2014, **43**, 15979; (f) K. Shen, M. Zhang and H. Zheng, *CrystEngComm*, 2015, **17**, 981.
10. (a) X. –H. Chang, Y. Zhao, M. –L. Han, L. –F. Ma and L. –Y. Wang, *CrystEngComm*, 2014, **16**, 6417; (b) L. Fan, X. Zhang, Z. Sun, W. Zhang, Y. Ding, W. Fan, L. Sun, X. Zhao and H. Lei, *Cryst. Growth Des.*, 2013, **13**, 2462; (c) X. Wang, L. Zhang, J. Yang, F. Liu, F. Dai, R. Wang and D. Sun, *J. Mater. Chem. A*, 2015,**3**, 12777; (d) X. –T. Zhang, L. –M. Fan, X. Zhao, D. Sun, D. – C. Li and J. –M. Dou, *CrystEngComm*, 2012, **14**, 2053; (e) J. Yang, X. Liu, X. Wang, F. Dai, Y. Zhou, B, Dong, L. Zhang, R. Liu and D. Sun, *Cryst. Growth Des.*, 2015, **15**, 4198; (f) L. Fan, W. Fan, B. Li, X. Liu, X. Zhao and X. Zhang, *CrystEngComm*, 2015, **17**, 4669.
11. (a) G. –W. Xu, Y. –P. Wu, H. –B. Wang, Y. –N. Wang, D. –S. Li and Y. –L. Liu, *CrystEngComm*, 2015,**17**, 9055; (b) L. Chen, L. Zhang, S. L. Li, Y. Q. Qiu, K. Z. Shao, X. L. Wang and Z. M. Su, *CrystEngComm*, 2013, **15**, 8214; (c) L. Fan, W. Fan, B. Li, X. Zhao and X. Zhang, *RSC Adv.*, 2015, **5**, 39854; (d) X. Li, F. Jiang, L. Chen, M. Wu, S. Lu, J. Pang, K. Zhou, X. Chen and M. Hong, *CrystEngComm*, 2016, **18**, 2239; (e) M. –L. Han, L. Bai, P. Tang, X. –Q. Wu, Y. –P. Wu, J. Zhao, D. –S. Li and Y. –Y. Wang, *Dalton Trans.,* 2015, **44**, 14673; (f) X. –T. Zhang, L. –M. Fan, W. –L. Fan, B. Li, G. –Z. Liu, X. –Z. Liu and X. Zhao, *Cryst. Growth Des.*, 2016, **16**, 3993.
12. (a) B. Liu, H. Miao, L. –Y. Pang, L. Hou, Y. –Y. Wang and Q. –Z. Shi, *CrystEngComm*, 2012, **14**, 2954; (b) B. Liu, L. Wei, N. Li, W. –P. Wu, H. Miao, Y. –Y. Wang and Q. –Z. Shi, *Cryst. Growth Des.*, 2014, **14**, 1110; (c) L. Fan, W. Fan, B. Li, X. Zhao and X. Zhang, *RSC Adv.*, 2015, **5**, 39854; (d) B. Liu, L. –Y. Pang, L. Hou, Y. –Y. Wang, Y. Zhang and Q. –Z. Shi, *CrystEngComm*, 2012, **14**, 6246; (e) B. Liu, L. Hou, Y. –Y. Wang, H. Miao, L. Bao and Q. –Z. Shi, *Dalton Trans.*, 2012, **41**, 3209; (f) D. Yan, R. Gao, M. Wei, S. Li, J. Lu, D. G. Evans and X. Duan, *J. Mater. Chem. C*, 2013, **1**, 997.
13. (a) J. P. S. Mowat, S. R. Miller, J. M. Griffin, V. R. Seymour, S. E. Ashbrook, S. P. Thompson, D. Fairen-Jimenez, A. Banu, T. Düren and P. A Wright, *Inorg. Chem.,* 2011, **50**, 10844; (b) X. –F. Wang, Y. –B. Zhang and Y. –Y. Lin, *CrystEngComm*, 2013, **15**, 3470; (c) S. B. Choi, H. Furukawa, H. J. Nam, D. Jung, Y. H. Jhon, A. Walton, D. Book, M. O'Keefe, O. M. Yaghi and J. Kim, *Angew. Chem. Int. Ed.,* 2012, **51**, 1; (d) S. S. Iremonger, R. Vaidhyanathan, R. K. Mah and G. K. H. Shimizu, *Inorg. Chem.*, 2013, **52**, 4124; (e) X. –F. Wang, Y. Wang, Y. –B. Zhang, W. Xue, J. –P. Zhang and X. –M. Chen, *Chem. Commun.,* 2012, **48**, 133; (f) D. Yan, G. O. Lloyd, A. Delori, W. Jones and X. Duan, *ChemPlusChem*, 2012, 77,1112.
14. (a) Y. –X. Ren, X. –J. Zheng, L. –C. Li, D. –X. Yuan, M. An and L. –P. Jin, *Inorg. Chem.*, 2014, **53**, 12234; (b) S. Horike, R. Matsuda, D. Tanaka, M. Mizuno, K. Endo and S. Kitagawa, *J. Am. Chem. Soc.*, 2006, **128**, 4222; (c) Y. –X. Ren, S. –S. Xiao, X. –J. Zheng, L. –C. Li and L. –P. Jin, *Dalton Trans.*, 2012, **41**, 2639; (d) A. Datta, K. Das, J. Lee, Y. Jhou, C. Hsiao, J. Huang and H. M. Lee, *CrystEngComm*, 2011, **13**, 2842; (e) Y. –X. Ren, X. –J. Zheng and L. –P. Jin, *CrystEngComm*, 2011, **13**, 5915; (f) Y. Tian, P. K. Allan, C. L. Renouf, X. He, L. J. McCormick and R. E. Morris, *Dalton Trans.*, 2014, **43**, 1519.
15. (a) G. M. Sheldrick, *SHELXTL*, version 5.1; Bruker Analytical X-ray Instruments Inc.: Madison, WI, 1998. (b) G. M. Sheldrick, *SHELX-97*, PC Version; University of Gottingen: Gottingen, Germany, 1997; (c) SMART, Saint and SADABS; Bruker AXS Inc.: Madison, Wisconsin, USA, 1998.
16. (a) V. A. Blatov, A. P. Shevchenko and V. N. Serezhkin, *J. Appl. Crystallogr.*, 2000, **33**, 1193; (b) V. A. Blatov, M. O'Keeffe and D. M. Proserpio, *CrystEngComm*, 2010, **12**, 44. (c) The network topology was evaluated by the program "TOPOS-4.0", see: http://www.topos.ssu.samara.ru.
17. (a) M. O'Keeffe, M. A. Peskov, S. J. Ramsden and O. M. Yaghi, *Acc. Chem. Res.*, 2008, **41**, 1782; (b) The Reticular Chemistry Structure Resource Database, see: http://rcsr.net/.
18. L. Yang, D. R. Powell and R. P. Houser, Dalton Trans., 2007, 955.
19. (a) A. L. Spek, *J. Appl. Crystallogr.*, 2003, **36**, 7; (b) A. L. Spek, *PLATON, A Multipurpose Crystallographic Tool*, Utrecht University, Utrecht, The Netherlands, 2002.
20. (a) X. Y. Wang, F. L. Jiang, L. Chen, J. Pan, K. Zhou, K. Z. Su, J. D. Pang, G. X. Lyu and M. C. Hong, *CrystEngComm*, 2015, **17**, 3829; (b) S. Yuan, Y. K. Deng, W. M. Xuan, X. P. Wang, S. N. Wang, J. M. Dou and D. Sun, *CrystEngComm*, 2014, **16**, 3829; (c) T. Liu, S. Wang, J. Lu, J. Dou, M. Niu, D. Li and J. Bai, *CrystEngComm*, 2013, **15**, 5476.
21. (a) Y. –Q. Mu, M. –L. Han, B. –H. Wang, W. Xia, W. –W. Dong and D. –S. Li, *Inorg. Chem. Commun.*, 2014, **46**, 259; (b) Y. Liu, H. Zhang, C. Tian, P. Lin and S. Du, *CrystEngComm*, 2013, **15**, 5201; (c) L. Liu, Y. –F. Peng, X. –X. Lv, K. Li, B. –L. Li and B. Wu, *CrystEngComm*, 2016, **18**, 2490; (d) Y. –L. Shao, Y. –H. Cui, J. –Z. Gu, A. M. Kirillov, J. Wu and Y. –W. Wang, *RSC Adv.*, 2015, **5**, 87484.
22. (a) T. Cao, Y. Peng, T. Liu, S. Wang, J. Dou, Y. Li, C. Zhou, D. Li and J. Bai, *CrystEngComm*, 2014, **16**, 10658; (b) Z. H. Yan, L. L. Han, Y. Q. Zhao, X. Y. Li, X. P. Wang, L. Wang and D. Sun, *CrystEngComm*, 2014, **16**, 8747; (c) L. Fan, W. Fan, B. Li, X. Liu, X. Zhao and X. Zhang, *RSC Adv.*, 2015, **5**, 14897.
23. (a) J. Pan, F. L. Jiang, M. Y. Wu, L. Chen, J. J. Qian, K. Z. Su, X. Y. Wan and M. C. Hong, *CrystEngComm*, 2014, **16**, 11078; (b) L. Fan, W. Fan, B. Li, X. Zhao and X. Zhang, *CrystEngComm*, 2015, **17**, 9413; (c) X. Zhang, L. Fan, W. Fan, B. Li and X. Zhao, *CrystEngComm*, 2015, **17**, 6681.
24. (a) M. –D. Zhang, L. Qin, H. –T. Yang, Y. –Z. Li, Z. –J. Guo and H. –G. Zheng, *Cryst. Growth Des.*, 2013, **13**, 1961; (b) X. Liu, Z. Xiao, A. Huang, W. Wang, L. Zhang, R. Wang and D. Sun, *New J. Chem.*, 2016, **40**, 5957; (c) L. Zhang, Y. Zhang, R. Wang, Z. Kang, X. Liu, D. Sun and G. Meng, *CrystEngComm*, 2015, **17**, 6591; (d) J. -M. Hao, B. –Y. Yu, K. V. Hecke and G. –H. Cui, *CrystEngComm*, 2015, **17**, 2279.
25. The Commission Internationale de l'Eclairage (CIE) colour coordinates were calculated based on the international CIE standards.
26. (a) M. Dai, H. –X. Li and J. –P. Lang, *CrystEngComm*, 2015, **17**, 4741; (b) J. Hao, B. Yu, K. V. Hecke and G. Cui, *CrystEngComm*, 2015, **17**, 2279; (c) Y. –F. Peng, S. Zhao, K. Li, L. Liu, B. –L. Li and B. Wu, *CrystEngComm*, 2015, **17**, 2544; (d) L. Liu, J. Ding, M. Li, Xi. Lv, J. Wu, H. Hou and Y. Fan, *Dalton Trans.*, 2014, **43**, 12790; (e) W. Y. Yin, Z. L. Huang, X. Y. Tang, J. Wang, H. J. Cheng, Y. S. Ma, R. X. Yuan and D. Liu, *New J. Chem.*, 2015, **39**, 7130; (f) C. –N. Lü, M. –M. Chen, W. –H. Zhang, D. –X. Li, M. Dai and J. –P. Lang, *CrystEngComm*, 2015, **17**, 1935; (g) H. –J. Chen, X. –Y. Tang, R. –X. Yuan and J. –P. Lang, *CrystEngComm*, 2016, **18**, 4851.

CrystEngComm

For Table of Contents Use Only

Table of Contents Graphic and Synopsis

Structural Diversity, Luminscence, and Photocatalytic Properties of Six Coordination Polymers Based on Designed Bifunctional 2-(1-imidazol-yl)terephthalic Acid

Xiutang Zhang, Liming Fan, Weiliu Fan, Bin Li, Guangzeng Liu, Xinzheng Liu and Xian Zhao

Based on the designed bifunctional 2-(1-imidazol-yl)terephthalic acid, six CPs were obtained with structural diversity and interestingly luminescence and photocatalytic properties.